# Combining RSM, Pareto Analysis, and EDAS for Multi-Objective Optimization of Turning Performance

**Nhat Tan Nguyen**
Vietnam-Japan Center, Hanoi University of Industry, Vietnam
tannn@haui.edu.vn

**Anh Thang Nguyen**
Vietnam-Japan Center, Hanoi University of Industry, Vietnam
thangna@haui.edu.vn

**Ngoc Linh Pham**
School of Mechanical and Automotive Engineering, Hanoi University of Industry, Vietnam
linhpn@haui.edu.vn (corresponding author)

*Received: 9 February 2026 | Revised: 13 April 2026 | Accepted: 25 April 2026*

 *DOI: https://doi.org/10.48084/etasr.18058*

**ABSTRACT**

**This study investigates the effects of cutting speed ($V_c$), feed rate ($f_z$), and depth of cut ($a_p$) on surface roughness ($R_a$) and Material Removal Rate (MRR) in turning operations. Fifteen experiments were conducted with $V_c$ ranging from 100 to 180 m/min, $f_z$ from 0.050 to 0.120 mm/rev, and $a_p$ from 0.050 to 0.200 mm. Analysis of Variance (ANOVA) revealed that $f_z$ is the most influential parameter on $R_a$, accounting for 49.69% of the total variation, while $V_c$ and $a_p$ show no statistically significant effects at the 95% confidence level. In contrast, MRR is significantly affected by all cutting parameters, with depth of cut contributing the most (54.27%), followed by $f_z$ (25.56%) and $V_c$ (12.31%). Logarithmic regression models were developed to describe the responses, yielding an adjusted coefficient of determination of 0.655 for $R_a$ and 1.000 for MRR. A multi-objective optimization problem was formulated to minimize $R_a$ and maximize MRR, and an extended Pareto front comprising nine non-dominated solutions was obtained. The Pareto solutions were ranked using the Evaluation based on Distance from Average Solution (EDAS) method, yielding the optimal compromise solution at a $V_c$ value of 180 m/min, $f_z$ equal to 0.085 mm/rev, and $a_p$ equal to 0.200 mm, with an $R_a$ value of 0.525 μm and an MRR value of 3060 mm³/min. The proposed framework effectively balances surface quality and productivity in turning operations.**

***Keywords-turning optimization; surface roughness; material removal rate; response surface methodology; pareto optimization; EDAS; multi-objective optimization; ANOVA***

## I. INTRODUCTION

Turning is one of the most significant machining processes in manufacturing, utilized for its simplicity and high productivity. The performance of turning is evaluated using two criteria: $R_a$ and MRR [1]. $R_a$ directly affects fatigue life, wear resistance, and dimensional accuracy. MRR represents productivity and influences manufacturing cost. Consequently, achieving high surface quality at acceptable productivity is a crucial challenge [2].

Machining parameters that improve surface quality reduce productivity, and vice versa. Lower $f_z$ produces smoother surfaces but significantly decreases MRR, whereas higher $f_z$ and depth of cut enhance material removal at the expense of surface finish [3, 4]. This inherent trade-off makes conventional single-objective optimization inadequate [5, 6]. Therefore, a multi-objective optimization framework that simultaneously minimizes $R_a$ and maximizes MRR is essential for practical applications.

The influence of cutting parameters on $R_a$ and MRR using statistical approaches has been investigated. ANOVA and regression models are frequently employed to identify significant parameters and describe relationships between cutting conditions and machining responses [5]. Response Surface Methodology (RSM) is capable of constructing predictive models with limited experiments and capturing nonlinear interactions among process parameters [1]. RSM-based models have been successfully applied to optimize surface roughness, tool wear, cutting forces, and productivity in turning [2, 7, 8].

To address the conflicting nature of machining objectives, various multi-objective optimization algorithms have been applied. Evolutionary algorithms such as the Genetic Algorithm (GA), Non-dominated Sorting Genetic Algorithm II (NSGA-II), and Particle Swarm Optimization (PSO) are widely used to generate Pareto-optimal solutions [9-11]. However, these algorithms often require large population sizes, multiple tuning parameters, and substantial computational effort. In contrast, Pareto-based optimization combined with response surface models provides a computationally efficient alternative [12, 13]. It directly identifies non-dominated solutions from model predictions or experimental results [6].

Once a Pareto front is obtained, the most appropriate compromise solution is selected. Various Multi-Criteria Decision-Making (MCDM) methods are employed to rank Pareto-optimal solutions in machining optimization, including TOPSIS, VIKOR, AHP, and MOORA [14-18]. However, many of these techniques rely on ideal and anti-ideal solutions or subjective pairwise comparisons. This introduces instability or bias, particularly when the number of Pareto solutions is limited.

The EDAS method is considered an effective MCDM technique [19]. Unlike conventional distance-based methods, EDAS evaluates alternatives by measuring their positive and negative distances from the average solution rather than from extreme ideal points. This characteristic makes EDAS less sensitive to outliers and more suitable for experimental machining data, where extreme values may arise due to process variability. Moreover, EDAS offers a simple mathematical structure and transparent interpretation.

This study proposes an integrated framework combining ANOVA, logarithmic regression modeling, Pareto-based multi-objective optimization, and EDAS ranking to optimize turning parameters. The effects of $V_c$, $f_z$, and depth of cut on $R_a$ and MRR are analyzed using ANOVA and regression models. An extended Pareto front is then constructed to represent the trade-off between surface quality and productivity. Finally, the EDAS method ranks Pareto-optimal solutions and identifies the optimal compromise cutting condition. The proposed approach provides a systematic tool for selecting turning parameters that balance surface finish and machining efficiency. Accordingly, this study develops an integrated ANOVA–RSM–Pareto–EDAS framework for optimizing turning performance in terms of surface quality and productivity.

## II. METHODOLOGY

The proposed methodology integrates statistical analysis, response surface modeling, and MCDM to optimize the turning process. The procedure consists of four main stages:

1. Statistical significance analysis using ANOVA
2. Development of regression models using RSM
3. Identification of Pareto-optimal solutions for conflicting objectives
4. Ranking of Pareto solutions using the EDAS method

This framework enables systematic assessment of cutting parameter effects and supports the selection of an optimal compromise solution between surface quality and productivity.

### *A. Response Surface Methodology*

RSM was employed to model the relationships between cutting parameters and machining responses. Although a second-order polynomial formulation is commonly used in RSM, logarithmic power-law models were adopted in this study due to the multiplicative nature of machining responses and their improved physical interpretability. The general form of the second-order RSM model is [13]:

$$Y = \beta_0 + \sum_{i=1}^{k} \beta_i x_i + \sum_{i=1}^{k} \beta_{ii} x_i^2 + \sum_{i=1}^{k-1} \sum_{j=i+1}^{k} \beta_{ij} x_i x_j \quad (1)$$

where $Y$ represents the response variable, $x_i$ denotes the coded independent variables, $\beta_0$ is the intercept term, $\beta_i$ are the linear coefficients, $\beta_{ii}$ are the quadratic coefficients, and $\beta_{ij}$ represent the interaction effects.

Considering the multiplicative nature of machining responses, a logarithmic transformation was applied to develop power-law models. The logarithmic form of the regression model is given by [19]:

$$\ln(Y) = \beta_0 + \beta_1 \ln(V_c) + \beta_2 \ln(f_z) + \beta_3 \ln(a_p) \quad (2)$$

By applying an exponential transformation, the model can be rewritten as:

$$Y = C \cdot V_C^{\beta_1} \cdot f_z^{\beta_2} \cdot a_p^{\beta_3} \quad (3)$$

where $C = \exp(\beta_0)$. This formulation provides a physically meaningful interpretation of the influence of each cutting parameter through the corresponding power exponent. The adequacy of the developed models was evaluated using the coefficient of determination ($R^2$), $R^2_{\text{adj}}$, F-statistic, and Root Mean Square Error (RMSE).

### *B. Pareto-Based Multi-Objective Optimization*

In practical turning operations, minimizing $R_a$ and maximizing MRR represent two conflicting objectives. Therefore, a multi-objective optimization problem was formulated:

$$min\ R_a(V_c, V_c, a_p), max MRR(V_c, V_c, a_p) \quad (4)$$

Instead of aggregating the objectives into a single scalar function, a Pareto-based approach was adopted to identify non-dominated solutions. A solution is considered Pareto-optimal if no other solution exists that simultaneously improves one objective without degrading the other. The resulting Pareto front represents the trade-off boundary between surface quality and productivity, and serves as the basis for subsequent decision-making.

### *C. Evaluation Based on Distance from Average Solution*

To select the most balanced cutting condition from the Pareto-optimal solutions, the EDAS method was employed. Let $x_{ij}$ denote the performance value of the $i$-th alternative with respect to the $j$-th criterion, and let $AV_j$ be the average value of the $j$-th criterion, defined as (5):

$$AV_j = \frac{1}{m}\sum_{i=1}^{m} x_{ij} \tag{5}$$

where $m$ is the number of Pareto-optimal alternatives. For benefit criteria, such as MRR, the positive and negative distances from the average solution are calculated by:

$$\begin{cases} PDA_{ij} = \max\left(0, \frac{x_{ij}-AV_j}{AV_j}\right) \\ NDA_{ij} = \max\left(0, \frac{AV_j-x_{ij}}{AV_j}\right) \end{cases} \tag{6}$$

For cost criteria, such as Ra, the expressions are reversed, as shown in:

$$\begin{cases} PDA_{ij} = \max\left(0, \frac{AV_j-x_{ij}}{AV_j}\right) \\ NDA_{ij} = \max\left(0, \frac{x_{ij}-AV_j}{AV_j}\right) \end{cases} \tag{7}$$

The weighted sums of positive and negative distances are then computed by:

$$\begin{cases} SP_i = \sum_{j=1}^{n} w_j \cdot PDA_{ij} \\ SN_i = \sum_{j=1}^{n} w_j \cdot NDA_{ij} \end{cases} \tag{8}$$

where $w_j$ denotes the weight of the $j$-th criterion and $n$ is the number of criteria. The normalized scores are obtained by:

$$\begin{cases} NSP_i = \frac{SP_i}{\max(SP_i)} \\ NSN_i = 1 - \frac{SN_i}{\max(SN_i)} \end{cases} \tag{9}$$

Finally, the EDAS appraisal score for the $i$-th alternative is calculated by:

$$AS_i = \frac{1}{2}(NSP_i + NSN_i) \tag{10}$$

Alternatives are ranked in descending order of $AS_i$, and the solution with the highest appraisal score is selected as the optimal compromise between $R_a$ and MRR.

The proposed RSM–Pareto–EDAS framework combines modeling accuracy, computational efficiency, and decision-making robustness. RSM provides predictive insights into the effects of the cutting parameters, the Pareto approach preserves the trade-off nature of conflicting objectives, and EDAS enables a stable and transparent ranking of optimal solutions. This integrated methodology is particularly suitable for turning experiments with limited datasets and provides practical guidance for selecting cutting conditions in industrial applications.

Although a second-order RSM formulation is introduced for generality, logarithmic power-law models were adopted due to the multiplicative nature of machining responses and their superior physical interpretability.

## III. EXPERIMENTAL PROCEDURE

### A. *Experimental Setup and Cutting Conditions*

The turning experiments were conducted on YK30 tool steel (JIS: SKS93), a high-carbon steel commonly used in the manufacture of cutting tools, dyes, and precision instruments. The chemical composition of YK30 steel is (wt.%): C 1.00–1.10, Si 0.15–0.50, Mn 0.60–1.10, Cr 0.10–0.50, P ≤ 0.030, S ≤ 0.030. After heat treatment, the workpiece achieved a hardness of 60÷65 HRC. Prior to machining, the workpiece surface was cleaned with acetone to remove oxide layers and contaminants, ensuring consistent cutting conditions.

All turning operations were performed on a DOOSAN Lynx 2100LY CNC lathe equipped with a FANUC 0i-TF Plus control system. Cubic Boron Nitride (CBN) cutting inserts with designation TNGA160404-CBN, grade CBN 1020, manufactured by LH Tools, were employed for all experiments. CBN is particularly suitable for machining hardened ferrous materials with a hardness above 45 HRC. The tool geometry included a nose radius of 0.4 mm, a relief angle of 7 °, and a negative rake angle of -6 °. The inserts were mounted on a CTGNR2525M16 tool holder. The experimental setup is illustrated in Figure 1.

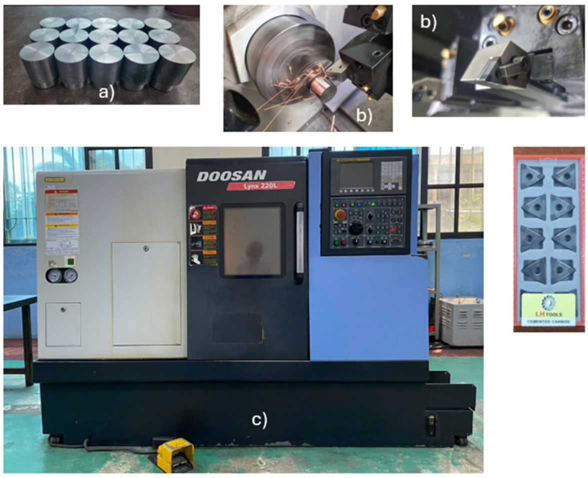


Fig. 1. Experimental setup. (a) YK30 workpiece (60 HRC), (b) CBN insert TNGA160404-CBN on tool holder, and (c) DOOSAN Lynx 2100LY CNC lathe.

To minimize the influence of tool edge wear on experimental results, a fresh CBN cutting edge was used for each experimental run. Visual inspection after each run confirmed that no significant flank wear ($V_B$ > 0.1 mm) was detected, ensuring that the recorded $R_a$ and MRR values reflect the influence of cutting parameters rather than tool degradation. Nevertheless, micro-scale edge rounding or chipping of the CBN insert, not detectable by visual inspection alone, could contribute to the unexplained variance in the Ra regression model. All experiments were performed under dry cutting conditions.

A Box–Behnken experimental Design (BBD) with 15 experimental runs was employed to investigate the effects of three cutting parameters: $V_c$, $f_z$, and $a_p$. The ranges of cutting parameters were established based on two criteria. First, the upper and lower bounds were set within the operational limits proposed by the CBN insert manufacturer (grade 1020) for finishing operations on hardened ferrous materials. Second, preliminary machining trials were conducted under selected conditions prior to the formal experiment to verify that all combinations within the chosen ranges produced measurable surface roughness values and did not cause premature tool failure. The center-point condition was validated in these trials, yielding $R_a$ between 0.516 and 0.518 µm, consistent with the replicated center-point results in the formal experiment. Three equally spaced levels were assigned to each parameter to satisfy the BBD requirements, as summarized in Table I.

TABLE I. CUTTING PARAMETERS AND THEIR LEVELS

| Symbol | -1 (low) | 0 (center) | 1 (high) |
|---|---|---|---|
| $V_c$ (m/min) | 100 | 140 | 180 |
| $f_z$ (mm/rev | 0.05 | 0.085 | 0.12 |
| $a_p$ (mm) | 0.05 | 0.125 | 0.2 |

In the BBD, each factor is studied at three levels; however, combinations corresponding to the extreme corners of the experimental domain are excluded.

### B. Data Analysis and Optimization Framework

The experimental data were analyzed using a structured statistical and optimization framework utilizing ANOVA to evaluate the significance and contribution of cutting parameters on both $R_a$ and MRR. Subsequently, logarithmic regression models were developed to describe the relationships between the cutting parameters and machining responses. The experimental design matrix and measured responses are presented in Table II.

TABLE II. EXPERIMENTAL DESIGN MATRIX AND MEASURED RESPONSES

| Run | $V_c$ (m/min) | $f_z$ (mm/rev) | $a_p$ (mm) | $R_a$ (µm) | MRR (mm³/min) |
|---|---|---|---|---|---|
| 1 | 100 | 0.050 | 0.125 | 0.259 | 625 |
| 2 | 140 | 0.050 | 0.050 | 0.364 | 350 |
| 3 | 100 | 0.085 | 0.200 | 0.983 | 1700 |
| 4 | 140 | 0.085 | 0.125 | 0.516 | 1488 |
| 5 | 140 | 0.050 | 0.200 | 0.403 | 1400 |
| 6 | 180 | 0.050 | 0.050 | 0.297 | 450 |
| 7 | 140 | 0.085 | 0.125 | 0.518 | 1488 |
| 8 | 140 | 0.085 | 0.125 | 0.516 | 1488 |
| 9 | 100 | 0.120 | 0.050 | 1.558 | 600 |
| 10 | 140 | 0.120 | 0.200 | 2.987 | 3360 |
| 11 | 100 | 0.050 | 0.050 | 0.271 | 250 |
| 12 | 180 | 0.050 | 0.125 | 0.237 | 1125 |
| 13 | 180 | 0.085 | 0.200 | 0.525 | 3060 |
| 14 | 100 | 0.120 | 0.200 | 3.128 | 2400 |
| 15 | 180 | 0.120 | 0.125 | 3.997 | 2700 |

$R_a$ was measured using a Mitutoyo SJ-301 portable surface roughness tester in accordance with ISO 4287. Three measurements were taken perpendicular to the cutting direction at different locations on the machined surface, and the average value was recorded. The sampling length was 0.8 mm with a cut-off length of 0.8 mm. MRR was calculated using:

$$MRR = 1000\, V_c\, f_z\, a_p \tag{11}$$

## IV. RESULTS AND DISCUSSION

### A. Statistical Analysis of Machining Responses

The ANOVA results for $R_a$ and MRR are outlined in Tables III and IV, respectively. The degrees of freedom for each case are set to two.

TABLE III. ANOVA RESULTS FOR SURFACE ROUGHNESS

| Source | Sum of squares | Mean square | p-value |
|---|---|---|---|
| $V_c$ | 1.2177 | 0.6089 | 0.3888 |
| $f_z$ | 5.9208 | 2.9604 | 0.036 |
| $a_p$ | 0.2043 | 0.1021 | 0.8396 |

The ANOVA resulted in non-significant effects of $V_c$ and $a_p$ with p-values of 0.3888 and 0.8396, respectively. $R_a$ in turning is primarily governed by the geometric mechanism expressed as $R_a \approx \frac{f_z^2}{8r}$, where the $f_z$ directly determines the height of the scallop left on the machined surface. Within the investigated range of $V_c$ (100–180 m/min), it primarily affects cutting temperature and tool–chip contact length rather than surface geometry, particularly when fresh cutting edges are used for each run. Similarly, the selected $a_p$ (0.05–0.20 mm) represents a typical finishing regime in which ap has a negligible geometric contribution to $R_a$ compared to $f_z$. These findings agree with [3, 4, 6]. The high p-values for $V_c$ and $a_p$ should not be interpreted as experimental error but as evidence of the $f_z$ dominance in the roughness formation mechanism. $f_z$ is the only statistically significant factor affecting $R_a$ at a 95% confidence level with a p-value of 0.036. $V_c$ and $a_p$ reveal no significant influence within the ranges investigated. Percentage contribution analysis confirms that $f_z$ accounts for 49.69% of the total variation in $R_a$, whereas $V_c$ and $a_p$ contribute 10.22% and 1.71%, respectively. This indicates that $R_a$ is primarily governed by feed-related geometric effects.

Figure 2 illustrates the relative importance of cutting parameters on $R_a$, with $f_z$ dominating. The minor contribution of $a_p$ suggests that its influence on surface finish is negligible compared to that of $f_z$ within the selected range.

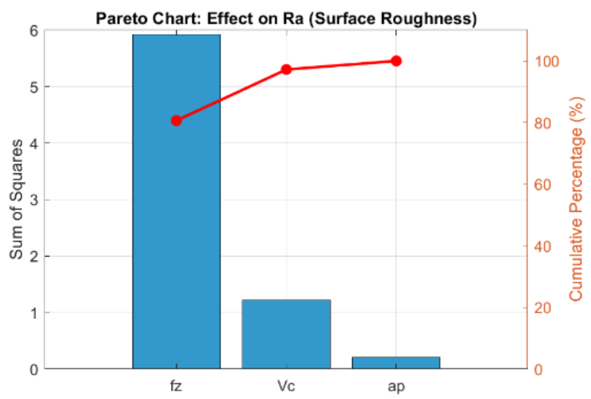


Fig. 2. Effect of cutting parameters on $R_a$.

In contrast to $R_a$, all three cutting parameters significantly affect MRR, as presented in Table IV. $a_p$ contributes the most

(54.27%), followed by $f_z$ (25.56%) and $V_c$ (12.31%). The degrees of freedom for each case are set to two.

TABLE IV. ANOVA RESULTS FOR MRR

| Source | Sum of squares | Mean square | p-value |
|---|---|---|---|
| $V_c$ | 1,445,000.23 | 722,500.12 | 0.0231 |
| $f_z$ | 3,001,250.23 | 1,500,625.12 | 0.0031 |
| $a_p$ | 6,372,450.23 | 3,186,225.12 | 0.0003 |

## B. Regression Modeling and Model Validation

To quantitatively describe the relationships between cutting parameters and machining responses, logarithmic regression models were developed as power-law equations. The estimated models for $R_a$ and MRR are summarized in Table V, and their predictive performance is evaluated in Figure 2.

TABLE V. LOGARITHMIC REGRESSION MODELS FOR SURFACE ROUGHNESS AND MRR

| | Percentage contribution (%) | | |
|---|---|---|---|
| **Variables** | $V_c$ | $f_z$ | $a_p$ |
| $R_a$ | 10.22 | 49.69 | 1.71 |
| MRR | 12.31 | 25.56 | 54.27 |

The logarithmic regression model for $R_a$ yields a moderate $R^2_{adj}$ of 0.655, suggesting that $R_a$ is influenced by additional factors such as tool wear or vibration. In contrast, the MRR model exhibits a perfect fit ($R^2_{adj} = 1.000$), consistent with its deterministic dependence on cutting parameters. On the contrary, the MRR model demonstrates an excellent fit with both $R^2$ and $R^2_{adj}$ equal to 1.0000. The predicted MRR values closely match the experimental data, confirming the deterministic relationship between MRR and cutting parameters.

## C. Pareto Front Analysis

Based on the experimental $R_a$ and MRR values, a multi-objective optimization problem was formulated to minimize $R_a$ while maximizing MRR. An extended Pareto front was constructed to identify non-dominated solutions, and the results are presented in Figure 3.

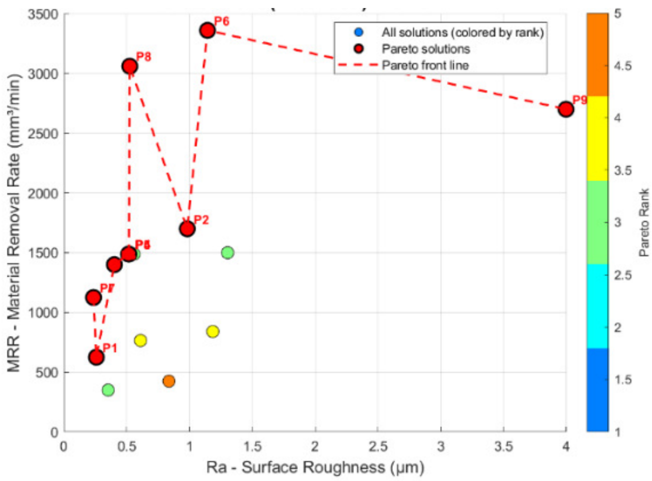


Fig. 3. Extended Pareto front illustrating the trade-off between $R_a$ and MRR obtained from experimental data.

Nine out of fifteen experimental solutions were identified as Pareto-optimal. The Pareto front illustrates the trade-off between surface quality and productivity. Solutions on the left exhibit lower $R_a$ but lower MRR, whereas those on the right achieve higher productivity at the expense of surface finish. This trade-off confirms that no single cutting condition can simultaneously minimize $R_a$ and maximize MRR.

## D. EDAS-Based Ranking of Pareto Solutions

To determine the most balanced cutting condition among the Pareto-optimal solutions, the EDAS method was applied. During the EDAS analysis, $R_a$ was treated as a cost criterion, whereas MRR was considered a benefit criterion. Equal weights were assigned to both criteria ($w_{Ra} = w_{MRR} = 0.5$). The EDAS ranking results are displayed in Table VI.

TABLE VI. EDAS RANKING OF PARETO-OPTIMAL SOLUTIONS

| No. | Index | $V_c$ (m/min) | $f_z$ (mm/rev) | $a_p$ (mm) | $R_a$ (μm) | MRR (mm³/min) | EDAS score (AS) | Rank |
|---|---|---|---|---|---|---|---|---|
| 1 | 14 | 180 | 0.085 | 0.200 | 0.525 | 3060 | 1 | 1 |
| 2 | 11 | 140 | 0.120 | 0.200 | 1.144 | 3360 | 0.8337 | 2 |
| 3 | 12 | 180 | 0.050 | 0.125 | 0.237 | 1125 | 0.7866 | 3 |
| 4 | 1 | 100 | 0.050 | 0.125 | 0.259 | 625 | 0.7343 | 4 |
| 5 | 5 | 140 | 0.050 | 0.200 | 0.403 | 1400 | 0.7285 | 5 |
| 6 | 8 | 140 | 0.085 | 0.125 | 0.516 | 1488 | 0.6807 | 6 |
| 7 | 7 | 140 | 0.085 | 0.125 | 0.518 | 1488 | 0.6797 | 7 |
| 8 | 3 | 100 | 0.085 | 0.200 | 0.983 | 1700 | 0.4799 | 8 |
| 9 | 15 | 180 | 0.120 | 0.125 | 3.997 | 2700 | 0.2019 | 9 |

The EDAS results indicate that the solution corresponding to Index 14 achieves the highest appraisal score and is ranked first. This optimal compromise solution is obtained at a $V_c$ value of 180 m/min, an $f_z$ of 0.085 mm/rev, and an $a_p$ of 0.200 mm, resulting in an $R_a$ of 0.525 μm and an $MRR$ of 3060 mm³/min. This cutting condition provides a favorable balance between surface quality and machining productivity.

To validate the robustness of the EDAS ranking, a sensitivity analysis was performed using three weighting scenarios:

- S1 with equal weights: $W_{R_a} = W_{MRR} = 0.5$
- S2 with priority to $R_a$: $W_{R_a} = 0.7$ and $W_{MRR} = 0.3$
- S3 with priority to MRR $W_{R_a} = 0.3$ and $W_{MRR} = 0.7$

The results are presented in Table VII. Across all three scenarios, the solution corresponding to Index 14 consistently achieves the highest appraisal score and retains Rank 1, confirming the robustness of the optimal solution regardless of the relative importance assigned to surface quality versus productivity. While intermediate rankings vary — notably, Index 11 drops from Rank 2 (S1) to Rank 7 (S2) when $R_a$ is prioritized, and Index 12 rises from Rank 3 (S1) to Rank 2 (S2) due to its low $R_a$ value — both the top-ranked and bottom-ranked solutions remain invariant across all scenarios.

TABLE VII. SENSITIVITY ANALYSIS OF EDAS RANKINGS UNDER VARIED CRITERION WEIGHTS

| Index | $R_a$ (μm) | MRR (mm³/ min) | S1 | Rank | S2 | Rank | S3 | Rank |
|---|---|---|---|---|---|---|---|---|
| 14 | 0.525 | 3060 | 1.000 | 1 | 0.977 | 1 | 1.000 | 1 |
| 11 | 1.144 | 3360 | 0.834 | 2 | 0.692 | 7 | 0.948 | 2 |
| 12 | 0.237 | 1125 | 0.787 | 3 | 0.973 | 2 | 0.550 | 4 |
| 1 | 0.259 | 625 | 0.734 | 4 | 0.940 | 3 | 0.447 | 8 |
| 5 | 0.403 | 1400 | 0.729 | 5 | 0.867 | 4 | 0.558 | 3 |
| 8 | 0.516 | 1488 | 0.681 | 6 | 0.791 | 5 | 0.544 | 5 |
| 7 | 0.518 | 1488 | 0.680 | 7 | 0.790 | 6 | 0.543 | 6 |
| 3 | 0.983 | 1700 | 0.480 | 8 | 0.489 | 8 | 0.460 | 7 |
| 15 | 3.997 | 2700 | 0.202 | 9 | 0.124 | 9 | 0.265 | 9 |

The ranking results demonstrate the effectiveness of the EDAS method in selecting a compromise solution from the Pareto front, avoiding bias toward extreme solutions with either very low $R_a$ or excessively high MRR.

### *E. Discussion*

It is acknowledged that dry cutting of hardened YK30 steel (60÷65 HRC) generates significant heat at the tool–workpiece interface [3, 4]. The elevated cutting temperature can induce thermal softening of the near-surface material, which may partially counteract the geometric roughness imposed by $f_z$, particularly at higher $V_c$. Additionally, thermal expansion of the workpiece could alter the effective depth of cut during machining. While these thermomechanical effects are not directly quantified in this study, they may contribute to the unexplained variance observed in the $R_a$ regression model ($R^2_{adj}$ = 0.655) and should be considered in future work involving in-situ temperature measurement.

The combined results of ANOVA, regression modeling, Pareto optimization, and EDAS ranking provide an understanding of the turning process. $f_z$ is identified as the dominant factor influencing $R_a$, while $a_p$ primarily governs MRR. The proposed multi-objective optimization framework successfully integrates statistical analysis and decision-making techniques to identify an optimal cutting condition that balances surface quality and productivity.

## V. CONCLUSION

This study presented an integrated Analysis of Variance (ANOVA), Response Surface Methodology (RSM), Pareto, and Evaluation based on Distance from Average Solution (EDAS) framework for multi-objective optimization of turning parameters on hardened YK30 steel (60÷65 HRC) using Cubic Boron Nitride (CBN) inserts under dry cutting conditions. The following conclusions were drawn:

1. ANOVA confirmed that feed rate ($f_z$) is the dominant factor affecting surface roughness $R_a$ (contribution: 49.69%; p = 0.036), while cutting speed ($V_c$) and depth of cut ($a_p$) showed no statistically significant influence within the investigated ranges, consistent with the geometric surface formation mechanism governing hard turning.
2. All three cutting parameters significantly affected Material Removal Rate (MRR), with $a_p$ being the primary driver (54.27%), followed by $f_z$ (25.56%) and $V_c$ (12.31%), reflecting MRR's direct proportionality to the product of all three parameters.
3. Logarithmic power-law regression models were successfully developed. The MRR model achieved a perfect fit ($R^2_{adj}$ = 1.000), whereas the $R_a$ model exhibited moderate accuracy ($R^2_{adj}$= 0.655), suggesting that additional influencing factors, such as thermomechanical effects and micro-scale tool edge conditions, warrant further investigation.
4. A Pareto front of nine non-dominated solutions was constructed, capturing the trade-off between surface quality and productivity. A sensitivity analysis of EDAS criterion weights, as presented in Table VII, confirmed the robustness of the optimal solution across varied weight distributions.
5. The EDAS method identified the optimal compromise cutting condition at $V_c$ equal to 180 m/min, $f_z$ to 0.085 mm/rev, and $a_p$ to 0.200 mm, yielding an $R_a$ value of 0.525 μm and an MRR of 3060 mm³/min. This is considered a practically viable condition, balancing surface finish and machining efficiency.

The proposed framework offers a systematic, computationally efficient approach for parameter selection in hard turning and is readily transferable to other machining processes. Future work should incorporate in-situ temperature measurement, quantitative tool wear monitoring, and validation under varied material conditions to further strengthen the model's predictive scope.

## DECLARATION OF COMPETING INTERESTS

The authors declare that there are no competing interests related to this publication.

## ACKNOWLEDGMENT

This research did not receive any specific funding from public, commercial, or non-profit organizations.

## DATA AVAILABILITY

The data used in this study are available from the corresponding author upon reasonable request.

## AI USE AND DECLARATION OF GENERATIVE AI USE

The authors used Generative AI only for checking grammar and improving the English writing of the manuscript. All technical contents, analysis, experimental results, and conclusions were carried out and verified by the authors.

## REFERENCES

[1] T. D. Nguyen, K. H. Nguyen, and L. N. Ha, "A Comparison of RSM-DA and PSO-TOPSIS in optimizing the Finishing Turning of 9XC Steel under MQL Conditions," *Engineering, Technology & Applied Science Research*, vol. 14, no. 3, pp. 14044–14048, June 2024, https://doi.org/10.48084/etasr.7100.

[2] N.-T. Nguyen, A.-T. Nguyen, R. M. Yue, V.-T. Pham, V.-L. Trinh, and V.-C. Nguyen, "Optimizing Turning Processes for SUS430C Steel: A Comparative Study of RSM and DFA Approaches," in *Proceedings of the 1st International Conference on Sustainability and Emerging Technologies for Smart Manufacturing*, Singapore, Singapore, 2025, pp. 591–599, https://doi.org/10.1007/978-981-97-7083-0_59.

[3] J. P. Davim, *Machining of Hard Materials*. Berlin, Germany: Springer Science & Business Media, 2011.

[4] F. Luis and G. Moncayo, *Metal Cutting Theory and Practice*, 3rd ed. Boca Raton, FL, USA: CRC Press, 2016.

[5] V. C. Nguyen, T. D. Nguyen, and D. H. Tien, "Cutting Parameter Optimization in Finishing Milling of Ti-6Al-4V Titanium Alloy under MQL Condition using TOPSIS and ANOVA Analysis," *Engineering, Technology & Applied Science Research*, vol. 11, no. 1, pp. 6775–6780, Feb. 2021, https://doi.org/10.48084/etasr.4015.

[6] Y. Su, G. Zhao, Y. Zhao, J. Meng, and C. Li, "Multi-Objective Optimization of Cutting Parameters in Turning AISI 304 Austenitic Stainless Steel," *Metals*, vol. 10, no. 2, Feb. 2020, Art. no. 217, https://doi.org/10.3390/met10020217.

[7] A. Johny and C. Thiagarajan, "Investigation of Surface Integrity and It's Optimization on Pure Titanium Using Molybdenum Wire by Reciprocated Travelling Wedm – A Review," *Materials Today: Proceedings*, vol. 33, pp. 2581–2584, Jan. 2020, https://doi.org/10.1016/j.matpr.2019.12.251.

[8] J. Jeykrishnan, B. V. Ramnath, C. Elanchezhian, and S. Akilesh, "Parametric Analysis on Electro-Chemical Machining of SKD-12 Tool Steel," *Materials Today: Proceedings*, vol. 4, no. 2, Part A, pp. 3760–3766, Jan. 2017, https://doi.org/10.1016/j.matpr.2017.02.272.

[9] C. N. Van, N. N. Ba, D. H. Tien, Q. N. Van, T. N. Xuan, and D. N. Thuy, "Using Support Vector Regression and Non-Dominated Sorting Genetic Algorithm in Multi-Objective Optimization of Milling of S50C Steel Under MQL Condition," *Journal of Applied Engineering Science*, vol. 20, no. 1, pp. 123–130, 2022, https://doi.org/10.5937/jaes0-31366.

[10] V. H. Pham, T. D. Nguyen, V. T. Le, D. H. Tien, and V.-C. Nguyen, "Optimization of Cutting Parameters in MQL Flat Surface Milling of SKD11 Steel," in *Proceedings of the International Conference on Advanced Mechanical Engineering, Automation, and Sustainable Development 2021 (AMAS2021)*, Cham, Switzerland, 2022, pp. 261–266, https://doi.org/10.1007/978-3-030-99666-6_40.

[11] V. T. Dang, V. T. Le, T. T. Nguyen, V. C. Nguyen, and V. L. Dao, "Multi-Criteria Decision-Making-Based Optimization of CMT-WAAM Process Parameters for SKD61 Steel Coating," *Welding International*, vol. 0, no. 0, pp. 1–26, Jan. 2026, https://doi.org/10.1080/09507116.2025.2610425.

[12] S. Nădăban, S. Dzitac, and I. Dzitac, "Fuzzy TOPSIS: A General View," *Procedia Computer Science*, vol. 91, pp. 823–831, Jan. 2016, https://doi.org/10.1016/j.procs.2016.07.088.

[13] K. Hinkelmann and O. Kempthorne, *Design and Analysis of Experiments*, vol. 2. Hoboken, NJ, United States: John Wiley & Sons, 2005.

[14] A. Mardani, A. Jusoh, K. M. Nor, Z. Khalifah, N. Zakwan, and A. Valipour, "Multiple Criteria Decision-Making Techniques and Their Applications – a Review of the Literature From 2000 to 2014," *Economic research - Ekonomska istraživanja*, vol. 28, no. 1, pp. 516–571, Dec. 2015, https://doi.org/10.1080/1331677X.2015.1075139.

[15] V. Q. Nguyen, H. T. Dung, V. T. Nguyen, V. D. Pham, and V. C. Nguyen, "Multiple Response Prediction and Optimization in Thin-Walled Milling of 6061 Aluminum Alloy," *Engineering, Technology & Applied Science Research*, vol. 13, no. 2, pp. 10447–10452, Apr. 2023, https://doi.org/10.48084/etasr.5667.

[16] V.-C. Nguyen, D.-T. Vu, Q.-H. Tran, V. Q. Kieu, and T. M. Nguyen, "Optimizing EDM for Titanium Alloys: An In-Depth Comparison of Five Mcdm Techniques.," *EUREKA: Physics & Engineering*, no. 5, Sep. 2024, Art. no. 89, https://doi.org/10.21303/2461-4262.2024.003283.

[17] A. Alinezhad and J. Khalili, "CRITIC Method," in *New Methods and Applications in Multiple Attribute Decision Making (MADM)*, A. Alinezhad and J. Khalili, Eds. Cham, Switzerland: Springer International Publishing, 2019, pp. 199–203.

[18] H. Taherdoost and M. Madanchian, "Multi-Criteria Decision Making (MCDM) Methods and Concepts," *Encyclopedia*, vol. 3, no. 1, pp. 77–87, Mar. 2023, https://doi.org/10.3390/encyclopedia3010006.

[19] R. H. Myers, D. C. Montgomery, and C. M. Anderson-Cook, *Response Surface Methodology: Process and Product Optimization Using Designed Experiments*. Hoboken, NJ, United States: John Wiley & Sons, 2016.